Collisions of Organic Molecules with Concentrated Sulfuric Acid: Scattering, Trapping, and Desorption

Jane K. Klassen,[†] Kathleen M. Fiehrer,[‡] and Gilbert M. Nathanson*

Department of Chemistry, University of Wisconsin, 1101 University Ave., Madison, Wisconsin 53706-1322

Received: July 17, 1997[⊗]

Molecular beam experiments demonstrate the diverse ways in which propane, propene, acetaldehyde, formic acid, dimethyl ether, and ethanol scatter from and react with 98.8 wt % H_2SO_4. The events following contact between gas and liquid include direct inelastic scattering from the acid's surface, trapping in the interfacial region followed by immediate desorption or desorption delayed by reversible protonation, and trapping followed by nearly irreversible protonation or further reaction. Molecules that scatter directly from the surface at incident and exit angles of 45° transfer from 70 to 80% of their impact energy of 90−110 kJ/mol. The fate of a molecule trapped at the interface depends on solute basicity and reactivity: the more basic molecules preferentially dissolve and undergo protonation rather than immediately desorb. Propane and propene desorb promptly, acetaldehyde and formic acid dissolve reversibly, and dimethyl ether and ethanol enter the acid for long times with little or no desorption following trapping. Substitution of 1-butanol for ethanol increases the size of the hydrophobic group but is insufficient to protect the OH group from protonation following thermal accommodation at the interface.

Introduction

The fate of organic molecules colliding into the surface of an acidic liquid such as H_2SO_4 depends both on the outcome of the initial collision and on the interfacial and solution phase reactivity of the molecule. Figure 1 illustrates four processes that may occur during a gas−liquid encounter.[1−5] The initial collision governs whether the incoming molecule scatters away from the surface (direct inelastic scattering) or whether it dissipates its energy via multiple collisions and binds momentarily to interfacial H_2SO_4 (trapping or accommodation). Gas molecules that are trapped in the interfacial region may then desorb immediately (trapping−desorption[6]) or remain long enough to become protonated in the interface or deeper in the bulk (trapping−reaction). Species that are protonated may remain in solution (long-time solvation) or react further,[7,8] or they may deprotonate and desorb from solution (trapping−reaction−desorption). Both immediate desorption and desorption delayed by reversible protonation generate thermal distributions of the evaporating parent molecules, so that H−D exchange[1] and residence time measurements[2] may be required to distinguish between the two channels.

Our previous studies provide direct evidence for the pathways in Figure 1. Scattering experiments show that impinging D_2O molecules either scatter directly from 98.8 wt % H_2SO_4 or become trapped at the interface and dissolve for times much longer than the 0.05 s measurement.[9] Formic acid molecules may also scatter inelastically, but those that accommodate undergo transient solvation followed by thermal desorption. Substitution of DCOOD for HCOOH generates desorbing DCOOH, revealing that accommodated formic acid molecules undergo solvation sufficient to cause proton exchange between DCOOD and H_2SO_4.[1] Additionally, uptake measurements show that the fraction of collisions leading to long-time protonation and further reaction of the oxygen-containing molecules in Table 1 increases steadily with the solution-phase basicity of the solute.[2] In all cases, the reaction probabilities decrease with increasing impact energy. This observation indicates that gas entry into the acid does not occur by "punching" through the surface but is limited by the fraction of molecules that can fully dissipate their energy to interfacial H_2SO_4.

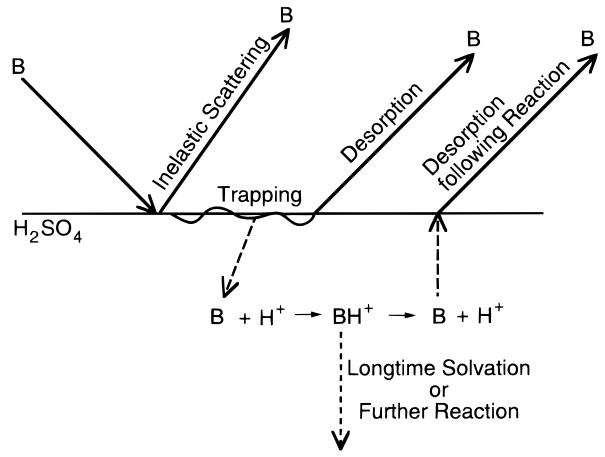

Figure 1. Possible pathways for a basic molecule B colliding into sulfuric acid. Protonation may occur in the interfacial or bulk regions of the acid.

We explore in this paper how scattering, trapping, reaction, and desorption compete in collisions of propane, propene, acetaldehyde, formic acid, dimethyl ether, and ethanol with 98.8 wt % H_2SO_4. This series of molecules was chosen because it spans a wide range of organic functional groups. Previous scattering experiments of rare gases from inert liquids indicate that the mass and size of the projectile, as well as its impact energy and angle of approach, can be important factors in controlling energy dissipation in gas−liquid collisions.[10−12] To separate these inertial effects from solute reactivity, we chose molecules of nearly equal size and mass and directed them at the surface of sulfuric acid at the same impact angle and nearly the same impact energy. Any significant differences in scattering will then primarily reflect differences in gas−surface

[†] Present address: Molecular Physics Laboratory, SRI International, 333 Ravenswood Ave., Menlo Park, CA 94025.

[‡] Present address: Intel Corporation, 5200 N. E. Elam Young Parkway, Hillsboro, OR 97124-6497.

[⊗] Abstract published in *Advance ACS Abstracts,* October 1, 1997.

S1089-5647(97)02329-8 CCC: $14.00

TABLE 1: Selected Properties of Six Organic Molecules

name	structure	mass (amu)	est size[a] (Å^3)	P[b] (Å^3)	C_{int}[c] (J/(mol/K))	$\Delta H°_{solv}(H_2O)$[d] (kJ/mol)	pK_{BH^+}[e]
propane	$CH_3CH_2CH_3$	44	150	6.4	53	−22	
propene	$CH_3CH{=}CH_2$	42	137	6.3	43	−28	≈−15
acetaldehyde	CH_3CHO	44	≈130	4.6	35	−33	−10
formic acid	HCOOH	46	≈130	>3.4	24	−47	−8.7
dimethyl ether	CH_3OCH_3	46	129	5.8	44	≈−40	−3.8
ethanol	CH_3CH_2OH	46	145	5.4	45	−53	−1.9

[a] van der Waals b constant $= RT_c/8P_c$. [b] Polarizability. [c] Heat capacity $C_{int} = C_{vib} + C_{rot} = C_P - 2.5R$. [d] Tabulated enthalpies of solvation of gas molecule in water. See ref 42. [e] p$K_{BH^+} = -\log K_{BH^+}$ for $BH^+ \leftrightarrow B + H^+$. Molecules are listed in order of increasing basicity. See ref 22.

TABLE 2: Selected Properties of Azeotropic Sulfuric Acid

concentration	94.0 mol %, 18.5 M, 98.8 wt % H_2SO_4
composition	88 mol % H_2SO_4, 6 mol % HSO_4^-, 6 mol % H_3O^+
density	1.83 g/cm^3
viscosity (25 °C)	24 cP
vapor pressure (25 °C)[a]	3.6, 3.1, 0.37, 0.16 × 10^{-5} Torr (total, H_2SO_4, H_2O, SO_3)
ΔH_{solv} (25 °C)[a]	−76 kJ/mol for $H_2O_{gas} \rightarrow H_2O_{azeotrope}$
boiling point[a]	315 °C
melting point[b]	3.3 °C
dielectric constant	≈102
dissociation constant	$2H_2SO_4 \leftrightarrow H_3SO_4^+ + HSO_4^-$, $K_{diss} = 10^{-3.6}$
H_0 (25 °C)[c]	−10.7
surface tension (20 °C)	54 dyn/cm

[a] Reference 17. [b] Kunzler, J. E.; Giaque, W. F. *J. Am. Chem. Soc.* **1952**, *74*, 5271. [c] Hammett acidity function, based on N protonation in aniline compounds. See ref 20.

attractive forces and gas reactivity in the interfacial and bulk regions, rather than kinematic effects during the collision itself. Table 1 confirms that the six molecules have nearly equal masses and sizes but that they differ widely in their ability to form hydrogen bonds (as gauged by their enthalpy of solvation in water) and in their basicity (pK_{BH^+}).

Selected properties of azeotropic sulfuric acid are listed in Table 2.[13,14] The 98.8 wt % (18.5 M) acid is composed mostly of neutral H_2SO_4 molecules, followed by 6 mol % each of H_3O^+ and HSO_4^-.[15,16] It is a low vapor pressure,[17] viscous liquid with a high dielectric constant, which can readily dissolve most salts and polar organic molecules.[8,14]

The protonating power of sulfuric acid is often gauged by its Hammett acidity function H_0, which is an extension of the pH scale for strong acids.[18,19] H_0 is −10.7 for 98.8 wt % H_2SO_4, in comparison with +7 for H_2O.[20] For many bases B, the ratio $[BH^+]/[B]$ can be roughly estimated from $\log\{[BH^+]/[B]\} \approx pK_{BH^+} - H_0$.[21] The function p$K_{BH^+} = -\log K_{BH^+}$ refers to the equilibrium constant for the deprotonation $BH^+ \leftrightarrow B + H^+$.[22] Less negative values of pK_{BH^+} reflect higher solution-phase basicities and larger $[BH^+]/[B]$ ratios. The last column of Table 1 indicates that p$K_{BH^+} - H_0$ is greater than zero for all species except propane and propene, implying that protonation should be extensive except for the hydrocarbons.

The solubility of oxygen-containing molecules in H_2SO_4 is driven by large enthalpies of protonation that favor conversion of B into BH^+. The total enthalpy of solvation at 25 °C for $H_2O(g)$ is −76 kJ/mol in azeotropic sulfuric acid, compared to −44 kJ/mol in liquid water. Tabulated solvation enthalpies in 92 wt % H_2SO_4 are −84 kJ/mol for ethanol, −78 kJ/mol for diethyl ether, and −73 kJ/mol for acetone.[23,24] These large negative enthalpies enforce low vapor solute pressures and long solvation times in the absence of further reactions. Arnett and co-workers have shown that the protonation enthalpies of many organic molecules in pure HSO_3F ($H_0 = -15$) scale linearly with pK_{BH^+}, suggesting that a similar relationship may hold for azeotropic H_2SO_4.[7]

The interfacial properties of sulfuric acid have been investigated by surface tension, Auger, and sum frequency generation (SFG) measurements. The surface tension of 98.8 wt % H_2SO_4 is ≈54 dyn/cm, in comparison with 73 dyn/cm for H_2O.[25] Because inorganic ions are less stable at the air−aqueous solution interface than in the bulk, the surface is likely to be populated by neutral H_2SO_4 species and not by H_3O^+ or HSO_4^-.[26] Auger analysis by Fairbrother et al. shows that the S and O content of interfacial H_2SO_4 mimics the bulk over a wide concentration range.[27] SFG studies by Radüge et al. further indicate that the OH groups of interfacial H_2SO_4 are hydrogen-bonded and lie parallel to the surface and that any residual dangling bonds must also lie in the surface plane.[28] The hydrogen bonds most likely bridge S−OH and O=S groups, perhaps in a layered structure that resembles the solid.[29] In addition, Gulden et al. have recently explored the reactivity of thin H_2SO_4 films in ultrahigh vacuum.[3] These experiments show that alcohols are readily absorbed by the acid and then dehydrate and desorb as olefins upon sublimation of the acid.

The time-of-flight (TOF) scattering experiments reported below show that the six molecules listed in Table 1 transfer nearly the same fraction of their incident energy during a direct inelastic collision. The fate of accommodated molecules, however, varies strongly with solution-phase basicity: weakly basic species that are trapped at the interface desorb from the acid before reaction occurs, while more basic species undergo solvation and long-time protonation or reaction. Even the presence of hydrophobic groups does not appear to alter the mechanism for solvation. Water, ethanol, and 1-butanol follow similar pathways upon collision: only impulsively scattered molecules escape dissolution into the acid.

Experiment

Clean and continuously renewed films of H_2SO_4 are produced using the techniques of Lednovich and Fenn.[9,30] Azeotropic sulfuric acid (98.8 wt %) is prepared by adding 106 wt % fuming H_2SO_4 (Aldrich) to 95 wt % H_2SO_4 (EM Science). The acid is degassed and heated in vacuum to 70 °C to approach the azeotrope more quickly. A 70 mL sample is then transferred to a Teflon reservoir inside the scattering chamber, and a 5.0 cm diameter vertical glass wheel is partially immersed in the acid at a liquid temperature, T_{liq}, of 295 K. The wheel rotates at 0.5 Hz, picking up a thin film of liquid whose outer portion is removed by a glass scraper. The resulting 0.3 mm thick film is exposed to the molecular beam through an 11 × 9.5 mm^2 hole for an exposure time $t_{exp} = 0.05$ s.

All scattering measurements were performed at incident and final angles of $\theta_i = \theta_f = 45°$, such that the mass spectrometer viewed a 4.5 × 3.2 mm^2 (umbra) area of the surface. For the data in Figures 2−4 and 6, the projected area of the molecular beam on the acid was 3.0 × 2.1 mm^2. The TOF spectra in Figure 5 were recorded using a larger projected beam area of 4.5 × 3.2 mm^2, and the exposure time was varied from 0.045 to 0.303 s by decreasing the rotation speed of the wheel. For

acetaldehyde and formic acid, the solvation times are on the order of t_{exp}, and the thermal desorption fractions (TD fractions) vary sensitively with beam area, detector viewing area, and t_{exp}.[31] The larger beam spot size used to produce Figure 5 limits the detector from viewing gas desorption from the rotating liquid outside the beam spot and thereby produces smaller TD fractions than in Figure 3. Reference 31 presents a quantitative analysis of the time dependence of the TD fractions for formic acid.

Molecular beams are created by expanding each gas through a 0.070 mm diameter heated nozzle at ≈1000 Torr. Table 3 lists the carrier gases and nozzle temperatures for each beam. High incident energies are created by expanding each gas in He or H_2 while lower energies are generated from expansions of the pure gases or by seeding in N_2. The nozzle is heated to suppress dimerization of ethanol and formic acid, producing incident beams that ionize in the mass spectrometer to yield monomer ion/dimer ion ratios, X^+/XH^+, exceeding 9:1. We estimate that the deposition rate is on the order of 0.3 monolayers/s for the seeded gases.

The TOF spectra were recorded using single-shot or cross-correlation techniques with the chopper wheels located between the liquid and doubly differentially pumped mass spectrometer and positioned 19.3 cm before the ionizer. Single-shot spectra (propene, propane) were recorded using an 18.0 cm diameter wheel spinning at 250 Hz with four 1.6 mm slots. The cross-correlation spectra were generated using a wheel etched with two pseudorandom sequences of 255 slots. The wheel was spun at 237 Hz, and the spectra were recorded in 8.25 μs time intervals. All TOF spectra have been corrected for electronic and timing offsets and for background signals at $m/e = 45$, 46, and 29 for the dimethyl ether, formic acid, and propane spectra, respectively. Background corrections were not necessary for ethanol or propene.

Results and Analysis

Time-of-Flight Analysis. The TOF spectra are plots of mass spectrometer signal $N(t)$ versus arrival time t at $\theta_i = \theta_f = 45°$. $N(t)$ is proportional to number density and is used to calculate the relative probability or flux, $P(E_f)$, that a molecule will scatter with translational energy E_f into angle θ_f. $P(E_f)$ is computed from the relations $P(E_f) \propto N(t)t^2$ and $E_f = (1/2)m_{gas}(L/t)^2$, where the flight path $L = 19.3 \pm 0.1$ cm.[32] All $P(E_f)$ distributions are obtained from direct inversion of the TOF spectra, typically resulting in errors in the average final energy $\langle E_f \rangle$ of less than 5%.

Figure 2 shows the TOF spectrum and energy distribution of propane scattering from H_2SO_4 at incident energy $E_i = 88$ kJ/mol. At high E_i, the $N(t)$ and $P(E_f)$ spectra are bimodal, corresponding to direct inelastic scattering (IS) at short arrival times (high recoil energies) and thermal desorption (TD) at long arrival times (low exit energies).[6,33,34] We assign the TD distribution to the component of $P(E_f)$ which falls within a Boltzmann distribution, $P_{TD}(E_f) = E_f(RT_{liq})^{-2}e^{-E_f/RT_{liq}}$. The IS distribution is assigned to the difference between $P(E_f)$ and $P_{TD}(E_f)$, normalized such that $P_{IS}(E_f) = 0$ at $E_f = RT_{liq} = 2.5$ kJ/mol. The TD fractions listed in Table 3 are then defined as the fraction of the scattered flux at $\theta_i = \theta_f = 45°$ which belongs to the TD distribution.

As Figure 2 shows, propane readily undergoes both inelastic scattering and thermal desorption. The incoming molecules typically lose ≈70% of their energy in direct scattering events, which account for 67% of the scattering intensity at $\theta_i = \theta_f = 45°$. We are unable to measure the net uptake of propane into the acid,[2] indicating that more than 99.9% of the incident molecules scatter or desorb from H_2SO_4 during the 0.05 s measurement time.

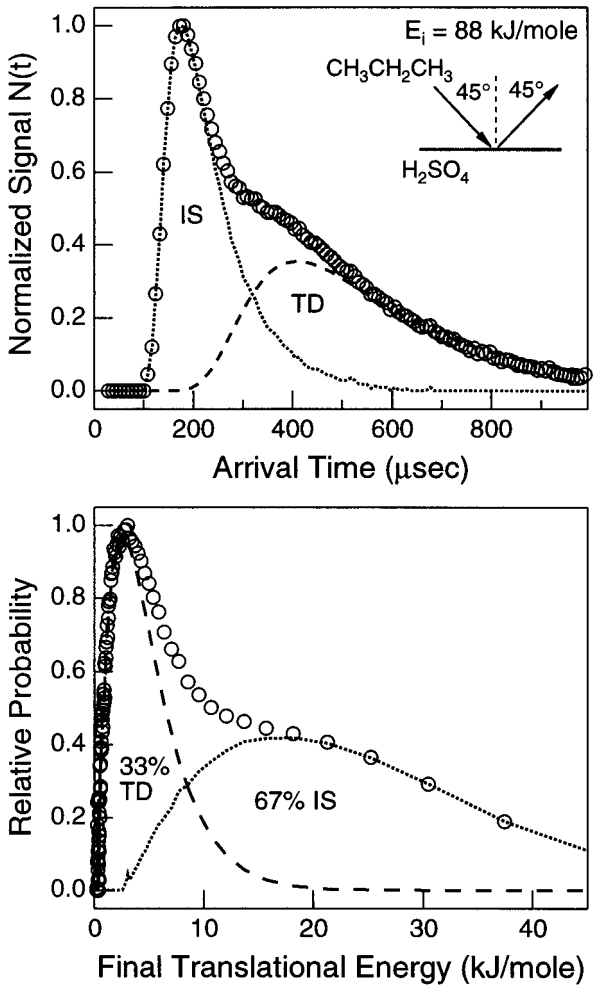

Figure 2. (a) Time-of-flight spectrum of propane scattering from 98.8 wt % H_2SO_4 at $\theta_i = \theta_f = 45°$. "IS" and "TD" refer to direct inelastic scattering and thermal desorption, respectively. (b) Relative probability $P(E_f)$ versus final translational energy E_f derived from the TOF spectrum.

High-E_i Time-of-Flight Spectra. Figure 3 displays TOF spectra of propene, acetaldehyde, formic acid, dimethyl ether, and ethanol at $E_i = 90-110$ kJ/mol and at $t_{exp} = 0.05$ s. The spectra are listed in order of increasing solution-phase basicity of the incident molecules. All spectra are normalized to one. The arrival times of the direct scattering components are similar in each case, with average fractional energy transfers ranging from 71% for propene to 79% for acetaldehyde (Table 3). The three least basic species—propene, acetaldehyde, and formic acid—each display substantial thermal desorption components. In contrast, the dimethyl ether and ethanol TOF spectra are dominated by direct scattering: the fractional contribution from thermal desorption is at most 10% and 7%, respectively. Uptake measurements shown in Figure 7 confirm that most dimethyl ether and ethanol molecules undergo long-time solvation in the acid. In these cases, the absence of a thermal desorption component indicates that trapping is followed by long-time solvation.

The effects of alkyl chain length can be examined by replacing ethanol with 1-butanol. Figure 4a shows scattering of $CH_3(CH_2)_3OH$ at $E_i = 187$ kJ/mol. A high incident energy is used to distinguish the IS and TD channels more clearly. Thermal desorption accounts for less than 2% of the signal, indicating that almost all of the accommodated butanol molecules dissolve in the acid for times longer than the 0.05 s observation time. To confirm that the high incident energy is

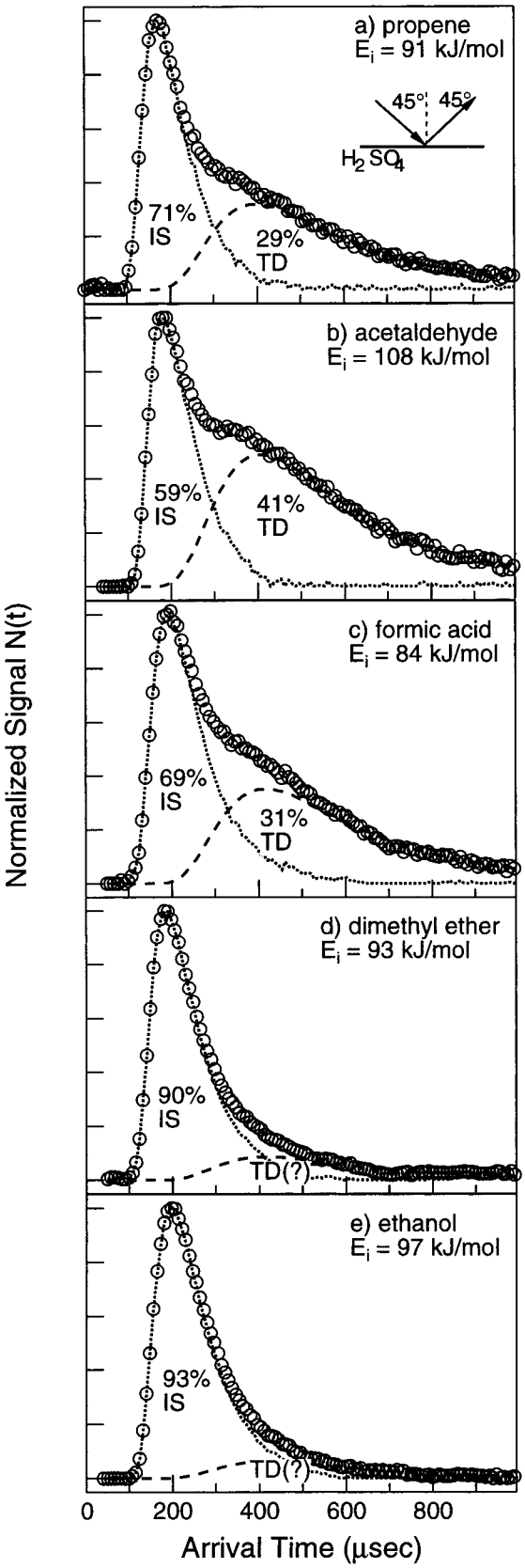

Figure 3. TOF spectra of propene, acetaldehyde, formic acid, dimethyl ether, and ethanol scattering from 98.8 wt % H_2SO_4 at exposure time $t_{exp} = 0.05$ s and at $\theta_i = \theta_f = 45°$.

not suppressing thermalization, we scattered 1-butanol from glycerol, $CH_2OHCH(OH)CH_2OH$, a strongly hydrogen-bonded liquid of low acidity. Panel b reveals the presence of a large desorption component and confirms that most molecules are thermalized during the collision.

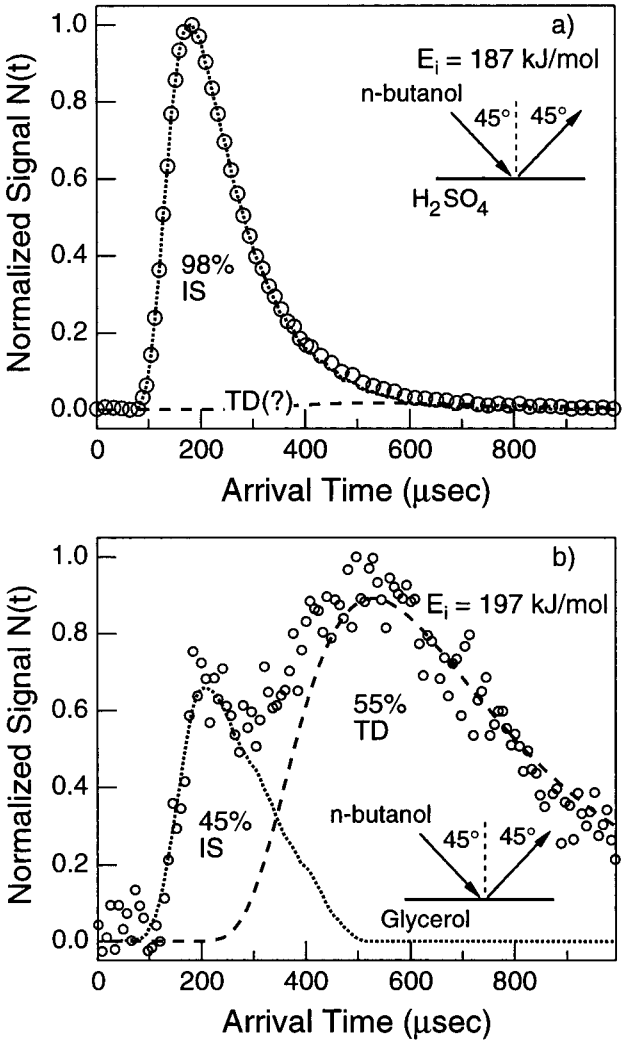

Figure 4. TOF spectra of 1-butanol scattering from (a) 98.8 wt % H_2SO_4 and (b) glycerol at $\theta_i = \theta_f = 45°$. The noise in the spectrum in panel b is caused by background subtraction of signal from evaporating glycerol at $m/e = 68$.

Exposure Time Dependence of TOF Spectra. At least three processes contribute to signal at long arrival times in the TOF spectra, where thermal desorption would occur: (1) desorption following long-time solvation and reversible protonation, (2) desorption immediately following accommodation at the surface, and (3) direct scattering events that leave the molecule with little kinetic energy. We can isolate the first contribution (the trapping−reaction−desorption channel) by measuring the average residence time of the gas molecule in the liquid. To determine residence times on the order of 10^{-2} to 10^{1} s, the rotation speed of the acid-covered wheel is varied to expose a patch of liquid on the surface to the incident gas for exposure times t_{exp} from 0.045 to 0.303 s.[2,31] At $\theta_i = \theta_f = 45°$, t_{exp} is roughly equal to the observation time of the rotating patch by the mass spectrometer. Molecules residing in the liquid for times less than t_{exp} will desorb and reach the mass spectrometer, while those undergoing solvation for times longer than t_{exp} will remain dissolved in the acid.[31] As the acid-covered wheel is rotated at slower speeds and t_{exp} is increased, more desorbing gas molecules will be viewed by the mass spectrometer, and the TD signal will grow.

Figure 5 shows TOF spectra of propene, formic acid, dimethyl ether, and ethanol at $t_{exp} = 0.045$ and 0.303 s. The spectra are not normalized within each panel. In every case, the inelastic scattering peak at short arrival times is independent of t_{exp}, as

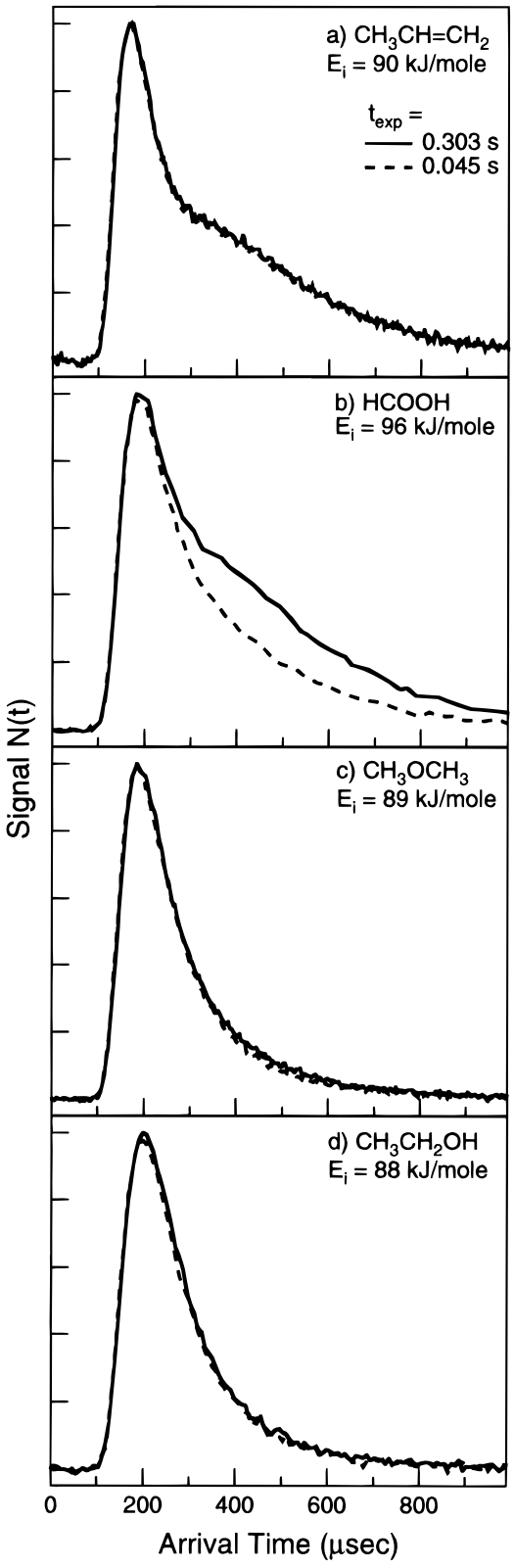

Figure 5. Dependence of the TOF spectra on t_{exp}, the exposure and observation time of a patch of surface on the rotating acid-covered wheel. In each spectrum, t_{exp} varies from 0.045 to 0.303 s. The spectra are not normalized within each panel. The sizes of the TD components in panel b are smaller than expected based on Figure 3c because of the 50% larger beam area used in these experiments and because of the higher incident energy.

expected for the subnanosecond duration of an impulsive collision. Panel a shows that the TD channel for propene is also independent of exposure time, indicating that the residence time for thermalized propene is much shorter than 10^{-2} s.

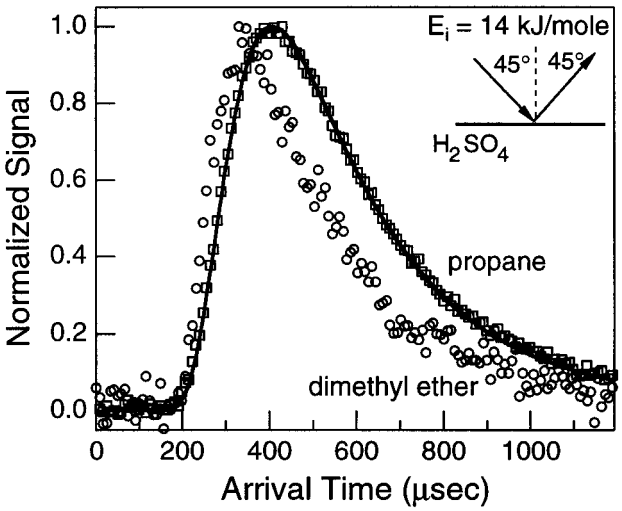

Figure 6. TOF spectra of dimethyl ether (○) and propane (□) scattering from 98.8 wt % H_2SO_4 at E_i = 14 kJ/mol and at $\theta_i = \theta_f = 45°$. The solid line is a Boltzmann distribution at mass 44 (propane) and T_{liq} = 295 K.

Separate experiments using 0.003 s pulsed beams of propene show pulse-limited rise and fall times, placing an upper limit on the residence time of thermalized molecules of $\approx 10^{-3}$ s.[35] The desorption component for formic acid, in contrast, increases by 65% from $t_{exp} = 0.045$ to 0.303 s. This change in TD signal with t_{exp} predicts a characteristic residence time on the order of 0.2−2 s.[2,31] Panel c reveals that the thermal desorption fraction for dimethyl ether increases slightly by 1−2% with t_{exp}, implying a many second residence time for dissolved CH_3OCH_3. This increase in thermal desorption is accompanied by a 0.5−1% decrease in dimethyl ether uptake over the same change in exposure times. We were unable to detect any time dependence to the long-time tail in the ethanol spectra in panel d. This result indicates that the weak ethanol TD signal is due either to low-energy inelastic scattering or to immediate thermal desorption following accommodation, but not to transient solvation on the time scale of $10^{-2}-10^{1}$ s.

Low-E_i TOF Spectra. Most experiments were performed with high incident energy molecules in order to distinguish more clearly between direct inelastic scattering and thermal desorption. The low-energy scattering results are in accord with the prediction of the high-E_i experiments. Figure 6 shows TOF spectra of dimethyl ether and propane scattering from H_2SO_4 at E_i = 14 kJ/mol or nearly 3 times the average thermal collision energy of $2RT_{liq}$ = 4.9 kJ/mol. The propane spectrum is fit well by a Maxwell−Boltzmann distribution at T_{liq} while the dimethyl ether spectrum is slightly faster than thermal, with an average final energy of 6.6 kJ/mol. The low-E_i ethanol and propene spectra resemble the dimethyl ether and propane spectra, respectively.[36]

The good agreement between the propane data and Boltzmann distribution indicates that most propane molecules are thermalizing and then desorbing and either that the IS channel is too weak to measure or that the velocities of most inelastically scattered molecules are dominated by thermal motions of the surface H_2SO_4 molecules. In contrast, the TOF spectra in Figures 3d and 5c show that thermalized dimethyl ether molecules do not desorb immediately. The TOF spectrum in Figure 6 should therefore be dominated by direct inelastic scattering. The dimethyl ether data are slightly faster than the Boltzmann curve because of limited energy transfer during direct scattering and because higher energy molecules in the incident beam are more likely to scatter than become trapped at the surface.[2]

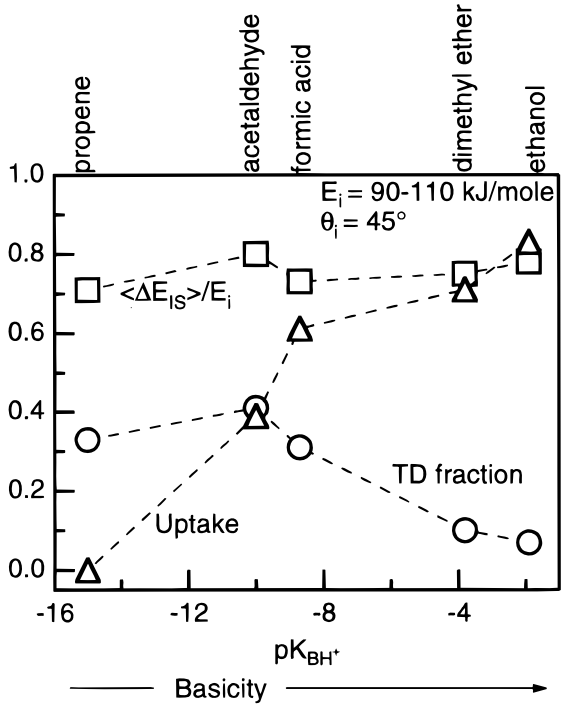

Figure 7. Plots of fractional energy transfer $\langle\Delta E_{IS}\rangle/E_i$ (□) and thermal desorption fractions (○) at $\theta_i = \theta_f = 45°$ and $E_i = 90-110$ kJ/mol versus the basicity (pK_{BH^+}) of each gas molecule. Gas uptake values (△) at $\theta_i = 45°$ are also shown. The exposure time t_{exp} is 0.05 s for all measurements: only the TD fractions and gas uptake values for acetaldehyde and formic acid depend substantially on t_{exp}.

Discussion

Figure 7 summarizes the TOF analysis for propene, acetaldehyde, formic acid, dimethyl ether, and ethanol striking 98.8 wt % acid as a function of solute basicity at $E_i = 90-110$ kJ/mol, $\theta_i = \theta_f = 45°$, and $t_{exp} = 0.05$ s. The fractional energy transfer in the inelastic scattering channel, $\langle\Delta E_{IS}\rangle/E_i$, is nearly constant at 70−80%. In contrast, the fraction of scattered molecules that undergo thermal desorption (TD fraction) varies from 29% for propene to 41% for acetaldehyde to less than 7% for ethanol. Figure 7 also displays the absolute gas uptake $S(\theta_i = 45°, t_{exp} = 0.045$ s) measured earlier,[2] which increases monotonically with the solution-phase basicity of the molecule. As discussed below, Figure 7 reveals an inverse trend between TD fractions and gas uptake.

The extent of scattering, trapping, and desorption depends on the efficiency of energy dissipation in the initial contact between the gas and acid and on the likelihood of protonation and further reaction of the accommodated molecules in the interfacial and bulk regions. In the sections below, we first discuss how energy dissipation in the inelastic channel depends on the identity of the gas molecule. We then analyze the thermal desorption channels and their relation to the interfacial and solution-phase reactivities of the organic molecules.

Inelastic Scattering. Table 3 lists the average energy transfers, $\langle\Delta E_{IS}\rangle/E_i$, and the normalized widths of the recoil energy distributions, $\pm\sigma_{IS}/E_i$. Energy transfer in the direct scattering channel is extensive, leaving each molecule on average with 20−30% of its initial energy. The widths of the $P_{IS}(E_f)$ range from ±10 to ±20% of E_i, generating broad distributions such as those shown in Figure 2 for propane. The spread in final energies likely reflects multiple collisions involving forward and backward deflections imposed by the corrugation of the surface and the irregular shapes of the gas and acid molecules, by thermal surface motions, and by attractive forces that deflect molecules toward the surface.[37,38]

The average fractional energy transfer for argon, the inert gas closest in mass to the organic molecules, is only 0.63. This value is 0.08−0.16 lower than the other $\langle\Delta E_{IS}\rangle/E_i$ entries in Table 3, indicating that the internal modes of the gas molecules and gas−surface attractive forces enhance energy transfer into the gas or acid by no more than 15% of the impact energy during a nonreactive trajectory. The relatively small variation in energy transfer among the six molecules reflects the similar kinematics for direct scattering of molecules of nearly equal mass and size.[39,40] To gauge the relative propensity for each molecule to absorb energy into their low-frequency vibrational modes, we list in Table 1 the values of the internal heat capacity $C_{int} = C_p - 2.5R$ at 300 K. There is little correlation between C_{int} and the small variations in $\langle\Delta E_{IS}\rangle/E_i$. In particular, energy transfer does not necessarily grow with the availability of low-frequency torsional or rocking modes,[41] since propane has the lowest torsional frequency of 200 cm^{-1} and the highest C_{int}, but a low $\langle\Delta E_{IS}\rangle/E_i$.

Table 1 also lists tabulated solvation enthalpies of each gas in water[42] as a relative measure of the attractive forces between the impinging gas and surface H_2SO_4 molecules prior to protonation.[32] The binding energies are weak for the hydrocarbon gases but strong where dipole−dipole forces and hydrogen bonding are possible. The $\Delta H°_{solv}(H_2O)$ correlate weakly with $\langle\Delta E_{IS}\rangle/E_i$: propane and propene are weakly attracted and transfer the least energy, while the oxygen-containing gases transfer more energy upon collision. We originally expected a more distinct change in $\langle\Delta E_{IS}\rangle/E_i$ with solute−solvent bond strength, since simple kinematic models predict that $\langle\Delta E_{IS}\rangle/E_i$ should scale with the strength of the gas−surface attractive potential V such that $\langle\Delta E_{IS}\rangle/E_i \propto (1 + V/E_i)$.[40] Benjamin and co-workers, however, show in a study of H_2O−glycerol collisions that the orientational constraints for hydrogen bonding are typically too strict for strong long-range attraction and that the initial gas−surface collision is similarly repulsive for trajectories leading to scattering or trapping.[38] H_2O molecules in the IS channel undergo further repulsive encounters, typically scattering away within 0.5 ps, while those in the TD channel remain behind, transferring their energy to a large number of glycerol molecules as the H_2O and glycerol begin to orient into hydrogen-bonding configurations.

The fractional energy transfer in the IS channel appears to be a relatively insensitive measure of changes in internal degrees of freedom (C_{int}), in hydrogen-bonding capability ($\Delta H°_{solv}$), or in the molecule's polarizability (Table 1). For the molecules listed in Table 1, the uniform $\langle\Delta E_{IS}\rangle/E_i$ values arise in part from the competition among these factors. This null effect may be a general characteristic for many-atom gas molecules possessing different functional groups. In certain cases, the values of $\langle\Delta E_{IS}\rangle/E_i$ may not be very sensitive to gas mass: even D_2O molecules at $E_i = 66$ kJ/mol lose 71% of their energy upon impact with sulfuric acid. The values of $\langle\Delta E_{IS}\rangle/E_i$ do reveal one important point: energy transfer is extensive during an impulsive encounter, one which typically involves one or a few bounces along the surface at high impact energy.[37,43] This efficient energy dissipation makes accommodation of the gas molecule in the interface a likely event and helps to explain the high measured uptake values and their weak dependence on impact energy.[2]

Trapping, Reaction, and Desorption. Impinging molecules that do not scatter directly from the surface are trapped at least momentarily at the interface.[37] The thermal desorption fractions reflect the likelihood for these accommodated molecules to desorb rapidly or after reversible protonation. In the three sections below, we describe the trends in TD fractions with

TABLE 3: Incident Beam Conditions, Fractional Energy Transfers, and Thermal Desorption Fractions

	incident beam conditions				final energy distribution		
molecule	carrier gas (temp,[a] K)	E_i (kJ/mol)	$E_i/\Delta E_i$ (fwhm)	M^+/D^+ [b]	$\langle \Delta E_{IS} \rangle / E_i$	$\pm \sigma_{IS}/E_i$ [c]	TD fraction
ethanol[d]	He (373)	97	5.2	19:1	0.78	±0.12	<0.07
	N_2 (373)	14	3.1	12:1			
dimethyl ether	H_2 (298)	93	6.7		0.75	±0.14	<0.10
	pure (298)	14	1.9				
formic acid[d]	He (473)	84	3.7	9:1	0.73	±0.16	0.31 (variable)
acetaldehyde	H_2 (298)	108	4.8		0.79	±0.11	0.41 (variable)
propene	H_2 (298)	91	7.0		0.71	±0.15	0.29
	pure (298)	13	2.1				
propane	H_2 (298)	88	7.1		0.72	±0.15	0.33
	pure (298)	14	1.9				
argon	H_2 (298)	90	12.1		0.63	±0.18	0.14

[a] Nozzle temperature. [b] Monomer ion/dimer ion ratio of ethanol and formic acid in the incident beam, monitored at X^+/XH^+. [c] $\pm \sigma_{IS}/E_i$ is the normalized width (±1 standard deviation/incident beam energy) of the inelastic component of the recoil energy distribution. [d] Reservoir temperatures are −9 °C (ethanol) and +9 °C (formic acid).

basicity, correlate gas uptake and TD values with specific reactions of each molecule, and speculate on the importance of interfacial protonation.

Trends with pK_{BH^+}. The TD fractions in Figure 7 first rise slightly and then fall with increasing solute basicity. This trend is in direct contrast with a previous study which showed that the TD fractions for Ne, CH_4, NH_3, and D_2O scattering from glycerol and the hydrocarbon squalane increase steadily with the free energy and enthalpy of solvation.[32] The primary difference between these systems is the ability of sulfuric acid to protonate and capture the solute molecules for long times. When the liquid is unreactive, all trapped molecules will desorb on the measurement time scale of >0.01 s, and the TD fractions will reflect the propensity for trapping. If the depth of the gas−surface attractive well scales with the bulk solvation energies, trapping and desorption will grow with ΔH_{solv}, as observed for glycerol and squalane. In contrast, protonation of the base B by H_2SO_4 in the interfacial or bulk regions delays desorption by the finite residence time of BH^+ in the acid.[2,5] This residence time increases for more basic molecules as protonation becomes more exothermic.[7] The extent of thermal desorption over a fixed observation time should therefore decrease with increasing basicity, as more molecules become protonated and remain behind rather than evaporate. This prediction is in accord with the inverse trends between thermal desorption fractions and gas uptake shown in Figure 7.

The gas uptake values and TD fractions furnish complementary information about the trapping process. The uptake coefficients provide an absolute measure of gas reactivity: S is the fraction of molecules that are captured by the acid at E_i and θ_i, and $(1 - S)$ is the fraction that scatter directly or undergo trapping and desorption into all exit angles. The high S values of 0.71 and 0.83 ± 0.03 at $\theta_i = 45°$ indicate that most impinging dimethyl ether and ethanol are trapped and dissolve for long times in the acid. The TD fractions in this case reveal which trajectories do not lead to reaction. In particular, the small TD fractions for ethanol and dimethyl ether in Figures 3, 5, and 6 show that the dominant escape route is by direct inelastic scattering and not by trapping followed by immediate desorption. Since ethanol and dimethyl ether desorption is minimal, the net uptake is close to the initial uptake or trapping probability leading to reaction. In contrast, propene displays very different behavior: greater than 99.9% of the propene molecules elude reaction with sulfuric acid, and at $\theta_f = 45°$, roughly half of the molecules escape by thermal desorption as by direct scattering. For molecules of intermediate basicity like acetaldehyde and formic acid, the TD flux and gas uptake depend on exposure time. In each case, the TD flux increases and the net gas uptake decreases at longer t_{exp} as solvated molecules desorb back into the vacuum. The time dependence of formic acid uptake indicates that the trapping probability leading to reaction is roughly 0.73, similar to that of dimethyl ether but lower than the value for ethanol.[31]

Functional Group Reactivity. The reaction channels following accommodation vary with functional group and determine the reversibility of protonation. For ethanol, we observe only long-time solvation: CH_3CH_2OH scattering from D_2SO_4 does not reveal evidence for H−D exchanged ethylene or ethanol.[35] This is in accord with cryoscopic and electrical conductivity measurements, which show in pure H_2SO_4 that ethanol is converted to ethyl hydrogen sulfate after protonation: $CH_3CH_2OH{\cdot}H^+ + H_2SO_4 \rightarrow CH_3CH_2OSO_3H + H_3O^+$.[13,44] We did not detect evaporating alkyl hydrogen sulfate, even though it is covalently bound.[45] The stability of this product is responsible in part for the long-time solvation of ethanol and its lack of time dependence in the TOF spectra in Figure 5d. The experiments of Roberts and co-workers suggest that we might detect gaseous ethylene if the acid was removed by evaporation or if it was heated and the observation times were longer.[3]

Figure 5c shows that accommodated dimethyl ether molecules also dissolve for long times in the acid. Cryoscopy[46] and NMR[47] studies indicate that dimethyl ether mostly undergoes simple protonation but may be cleaved to generate methyl hydrogen sulfate at high temperatures or long reaction times.[8,46] The 1−2% change in thermal desorption from $t_{exp} = 0.045$ to 0.303 s corresponds to a many second average residence time, reflecting the basic character of the ether. Acetaldehyde also undergoes reversible protonation and desorption, but on a much faster time scale of ≈0.1 s because of its lower basicity.[2,8,48] Although we did not record spectra of acetaldehyde as a function of t_{exp}, the trends in Figure 5 suggest that its TD component is larger than for dimethyl ether because of this reversible protonation and desorption.

The reversible solvation of formic acid, shown in Figure 5b, most likely occurs through protonation and deprotonation at the carbonyl group, generating a resonance-stabilized intermediate $HC(OH)_2^+$.[18,49] The primary irreversible path is decomposition into H_3O^+ and CO,[50] which may occur via protonation at the OH rather than the C═O group.[18] We observe only a weak CO thermal desorption signal from formic acid, hidden in part by residual N_2 and by dissociative ionization of HCOOH at $m/e = 28$. Preliminary reactive uptake measurements indicate that this CO channel is weak, with a reaction probability estimated to be below 5% under our conditions.[31,51]

Propene dissolves exothermically in concentrated sulfuric acid[52] to generate isopropyl hydrogen sulfate, but the reaction is inhibited by a high activation energy.[53] We were unable to detect any uptake at accessible measurement times of 10^{-3} s or

longer. The large thermal desorption component in Figure 3a shows that this lack of reactivity is not because the molecule is unable to dissipate its energy, but because it desorbs faster than it can dissolve and react.

The TOF spectra cumulatively demonstrate that thermal desorption intensities generally decrease as the solution-phase basicity increases. The near absence of desorption (ethanol, dimethyl ether) correlates with nearly irreversible absorption over the time scale of $10^{-2}-10^{1}$ s, while changes in the thermal desorption flux with exposure time (formic acid) reflect reversible protonation and desorption of the solute molecule. Substantial TD signals that are independent of time (propene, propane) in our experiments indicate that no interfacial or bulk reactions are occurring and that desorption occurs on time scales shorter than 10^{-3} s.

Interfacial versus Bulk Protonation. The first steps in long-time solvation appear to be similar for water and alcohols, including D_2O,[9] CH_3CH_2OH, and $CH_3CH_2CH_2CH_2OH$. In each case, there is little or no evidence for thermal desorption, indicating that nearly all accommodated molecules enter the bulk: the only immediate escape route is by direct scattering from the surface. This result implies that mechanical energy dissipation almost always leads to interfacial residence times long enough to allow H_2SO_4 molecules to bind to each ROH molecule before it desorbs. Even hydrophobic groups as large as *n*-butyl do not act as protecting groups during the thermalization process. This efficient binding may proceed first by attractive interactions when the ROH group comes in contact with lone pairs of the O atoms of surface S═O or S−OH groups, followed by switching from interfacial S−OH···O═S to S−OH···OHR hydrogen bonds that act as a bridge for proton transfer from sulfuric acid to the O atom of ROH.[28,54]

The ethanol TOF spectra provide an estimate of the timing and location of protonation. The near absence of any desorption of trapped ethanol molecules implies that they must be protonated quickly compared to their characteristic residence times for physical (nonreactive) solvation, since they would otherwise depart before reacting. A characteristic residence time τ for physical solvation can be estimated from $\tau = D(4HRT/\alpha\langle v\rangle)^2 \approx 10^{-7}$ s, where the diffusion coefficient is $D \approx 5 \times 10^{-7}$ cm^2/s,[55] the Henry's law constant is $H \approx 200$ M/atm for physical solvation,[56] the initial uptake is $\alpha \approx 1$, and the thermal gas velocity is $\langle v\rangle \approx 4 \times 10^4$ cm/s.[5,57] During this 10^{-7} s solvation time, the molecule may diffuse a distance of roughly $(\pi D\tau)^{1/2} \approx 50$ Å. The ethanol TOF spectrum shows that no more than 7% of the scattered molecules at $\theta_i = \theta_f = 45°$ are due to desorption from the acid after accommodation. The uptake measurements further show that, at $E_i = 90$ kJ/mol and at $\theta_i = 45°$, the capture probability is 0.83. If scattering at $\theta_i = \theta_f = 45°$ is typical of the overall collision process, then the maximum fraction of trapped molecules that desorb is $0.07 \times (1 - 0.83) \approx 1\%$. The remaining 99% of the accommodated ethanol molecules undergo protonation and long-time solvation. The typical time and depth for reaction to occur in order to observe a maximum 1% desorption must be much smaller than the physical solvation values of 10^{-7} s and 50 Å, implying that protonation is likely to occur near the interfacial region and on nanosecond or smaller time scales.[58] Thus, it seems likely that sulfuric acid can sufficiently solvate alcohols (and likely ethers and carboxylic acids) for protonation to take place near the surface region.

Conclusions

Collisions of propane, propene, acetaldehyde, formic acid, dimethyl ether, and ethanol with 98.8 wt % sulfuric acid demonstrate many of the possible pathways in reactive gas−reactive liquid encounters. At $E_i = 90-110$ kJ/mol and at $\theta_i = \theta_f = 45°$, each molecule is observed to scatter inelastically from the surface or transfer its energy completely to the acid and thermalize. Energy transfer in the inelastic scattering channel is extensive for all molecules, exceeding at least two-thirds of their impact energy. The events occurring after thermalization are best predicted by the solution-phase basicity of the gas molecule, as gauged by its pK_{BH^+} for the reaction $BH^+ \leftrightarrow B + H^+$. The more basic species (more positive pK_{BH^+}) will be protonated by the acid for longer times following accommodation. This protonation delays desorption or promotes further reaction. Thermal desorption rates therefore drop, and long-time gas uptake grows as pK_{BH^+} increases.

Despite the extreme protonating power of azeotropic sulfuric acid, even very basic molecules can survive collisions with the acid at low and high impact energies. The dominant route to escape solvation is by direct inelastic scattering: molecules that thermalize at the interface almost always undergo at least transient solvation if they are soluble. This scenario is most compelling for water, alcohols, and ethers, which undergo very long-time solvation, and for carboxylic acids, which mostly undergo proton exchange before desorbing.[1] The absence of almost any desorbing ROH species following trapping indicates that protonation of the −OH group occurs very near the interface, implying that interfacial sulfuric acid is itself a strong protonating medium. For reactive gases striking an acidic liquid, the trapping process appears to be the rate-limiting step in the initial solvation of an impinging molecule, while the solution-phase basicity controls its ultimate fate.

Acknowledgment. We are grateful to the National Science Foundation for funding this work under Grant CHE-9417909. We thank Y. T. Lee for permission to reproduce his cross-correlation wheels, B. Ringeisen for recording the 1-butanol/glycerol TOF spectrum, and G. P. Miller for discussions concerning ethanol protonation.

References and Notes

(1) Klassen, J. K.; Nathanson, G. M. *Science* **1996**, *273*, 333.
(2) Fiehrer, K. M.; Nathanson, G. M. *J. Am. Chem. Soc.* **1997**, *119*, 251.
(3) Guldan, E. D.; Schindler, L. R.; Roberts, J. T. *J. Phys. Chem.* **1995**, *99*, 16059.
(4) For H_2O collisions with ice, see: Brown, D. E.; George, S. M.; Huang, E. K.; Wong, E. K. L.; Rider, K. B.; Smith, R. S.; Kay, B. D. *J. Phys. Chem.* **1996**, *100*, 4998.
(5) See, for example: Jayne, J. T.; Worsnop, D. R.; Kolb, C. E.; Swartz, E.; Davidovits, P. *J. Phys. Chem.* **1996**, *100*, 8015. Lovejoy, E. L.; Hanson, D. R. *J. Phys. Chem.* **1996**, *100*, 6397.
(6) Hurst, J. E.; Becker, C. A.; Cowin, J. P.; Janda, K. C.; Wharton, L.; Auerbach, D. J. *Phys. Rev. Lett.* **1979**, *43*, 1175.
(7) Arnett, E. M.; Scorrano, G. *Adv. Phys. Org. Chem*. **1976**, *13*, 83. Arnett, E. M.; Mitchell, E. J.; Murty, T. S. S. R. *J. Am. Chem. Soc.* **1974**, *96*, 3875.
(8) Gillespie, R. J.; Leisten, J. A. *Q. Rev.* **1954**, *8*, 40.
(9) Govoni, S. T.; Nathanson, G. M. *J. Am. Chem. Soc.* **1994**, *116*, 779.
(10) Saecker, M. E.; Nathanson, G. M. *J. Chem. Phys*. **1993**, *99*, 7056.
(11) King, M. E.; Nathanson, G. M.; Hanning-Lee, M. A.; Minton, T. K. *Phys. Rev. Lett.* **1993**, *70*, 1026.
(12) Ronk, W. R.; Kowalski, D. V.; Manning, M.; Nathanson, G. M. *J. Chem. Phys.* **1996**, *104*, 4842.
(13) Gillespie, R. J.; Robinson, E. A. In *Non-Aqueous Solvents*; Waddington, T. C., Ed.; Academic Press: New York, 1963; p 117.
(14) Lee, W. H. In *The Chemistry of Non-Aqueous Solvents*; Lagowski, J. J., Ed.; Academic Press: New York, 1967; Vol. II, p 99.
(15) Cox, R. A. *J. Am. Chem. Soc.* **1974**, *96*, 1059.
(16) Robertson, E. B.; Dunford, H. B. *J. Am. Chem. Soc.* **1964**, *86*, 5080.
(17) Bolsaitis, P.; Elliot, J. F. *J. Chem. Eng. Data* **1990**, *35*, 69.
(18) Liler, M. *Reaction Mechanisms in Sulfuric Acid*; Academic Press: New York, 1971.

(19) Rochester, C. H. *Acidity Functions*; Academic Press: New York, 1970.

(20) Johnson, C. D.; Katritzky, A. R.; Shapiro, S. A. *J. Am. Chem. Soc*. **1969**, *91*, 1, 6654.

(21) The Hammett Acidity function is given by $H_0 = -\log(a_{H^+}f_{BH^+}/f_B)$ where *a* is an activity and *f* is an activity coefficient.

(22) pK_{BH^+} values for weak bases are difficult to measure and are sometimes determined as the value of H_0 where $[BH^+] = [B]$. In these cases, K_{BH^+} may not be a true equilibrium constant. For specific values, see: Lee, D. G.; Cameron, R. *J. Am. Chem. Soc*. **1971**, *93*, 4274 (ethanol). Arnett, E. M.; Wu, C. Y. *J. Am. Chem. Soc.* **1962**, *84*, 1680 (dimethyl ether): Reference 18 (formic acid). Levy, G. C.; Cargioli, J. D.; Racela, W. *J. Am. Chem. Soc.* **1970**, *92*, 6238 (acetaldehyde). Arnett, E. M.; Hofelich, T. C. *J. Am. Chem. Soc.* **1983**, *105*, 2889; Arnett, E. M.; Petro, C. *J. Am. Chem. Soc.* **1978**, *100*, 5408 (propene, rough estimate on H_R' scale).

(23) Arnett, E. M.; Burke, J. J.; Carter, J. V.; Douty, C. F. *J. Am. Chem. Soc*. **1972**, *94*, 8737. The value for diethyl ether was measured in 96 wt % acid. In comparison, the solvation enthalpy for water drops from −75 to −72 kJ/mol in 96 wt % to 92 wt % H_2SO_4.

(24) The solvation enthalpy of propane in 93 wt % sulfuric acid is listed as −9 kJ/mol. Rudakov, E. S.; Lutsyk, A. I. *Zh. Fiz. Khim.* **1979**, *43*, 1298.

(25) *International Critical Tables;* Washburn, E. W., Ed.; McGraw-Hill: New York, 1928; Vol. 4, p 464. Sabinina, L.; Terpugow, L. *Z. Phys. Chem*. (*Munich*) **1935**, *A173*, 237.

(26) Eisenthal, K. B. *Acc. Chem. Res* **1993**, *26*, 636. Benjamin, I. *J. Chem. Phys*. **1991**, *95*, 3698. Phillips, L. F. *Aust. J. Chem.* **1994**, *47*, 91.

(27) Fairbrother, D. H.; Johnston, H.; Somorjai, G. *J. Phys. Chem.* **1996**, *100*, 113696.

(28) Radüge, C.; Pflumio, V.; Shen, Y. R. *Chem. Phys. Lett.* **1997**, *274*, 140. See also: Baldelli, S.; Schnitzer, C. S.; Schultz, M. J.; Campbell, D. J., submitted to *J. Phys. Chem.*

(29) Kemintz, E.; Werner, C.; Trojanov, S. *Acta Crystallogr*. **1996**, *C52*, 2665.

(30) Lednovich, S. L.; Fenn, J. B. *AIChE J*. **1977**, *23*, 454.

(31) Fiehrer, K. M.; Ringeisen, B. R.; Nathanson, G. M. Manuscript in preparation.

(32) Saecker, M. E.; Nathanson, G. M. *J. Chem. Phys*. **1993**, *99*, 7056.

(33) We previously used the abbreviation "TD" to refer to trapping−desorption. In the presence of both nonreactive and reactive gas−liquid interactions, it is clearer to redefine "TD" as thermal desorption, which refers to the observation of a thermal distribution in the TOF spectra. "Trapping−desorption" then specifically refers to the process of trapping, no reaction, and thermal desorption. "Trapping−reaction−desorption" refers to the process of trapping, reaction at the interface or bulk, followed by thermal desorption.

(34) Rettner, C. T.; Schweizer, E. K.; Mullins, C. B. *J. Chem. Phys*. **1989**, *90*, 3800.

(35) Fiehrer, K. M. Ph.D. Thesis, University of Wisconsin, 1997.

(36) Klassen, J. K. Ph.D. Thesis, University of Wisconsin, 1995.

(37) Benjamin, I.; Wilson, M.; Pohorille, A. *J. Chem. Phys*. **1994**, *100*, 6500. Barker, J. A.; Auerbach, D. J. *Faraday Discuss. Chem. Soc*. **1985**, *80*, 277. Lim, C.; et al. *J. Chem. Phys*. **1987**, *87*, 1808.

(38) Benjamin, I.; Wilson, M. A.; Pohorille, A.; Nathanson, G. M. *Chem. Phys. Lett.* **1995**, *243*, 222.

(39) This result is in accord with kinematic models for single collision energy transfer, which predicts that $\Delta E_{IS}/E_i = f(\mu,\chi)(1 + V/E_i)$, where $\mu = m_{gas}/m_{surface}$, $\chi = 180° - (\theta_i + \theta_f)$ is the angle of deflection, $f(\mu,90°) = 2\mu/(1 + \mu)$, and *V* is the depth of the attractive potential. For molecules of nearly equal size and mass scattering at $\theta_i = \theta_f = 45°$, *f* should be nearly constant.

(40) Harris, J. In *Dynamics of Gas-Surface Interactions*l; Rettner, C. T., Ashfold, M. N. R., Eds.; Royal Society of Chemistry: Cambridge, 1991; p 1. Grimmelmann, E. K.; Tully, J. C.; Cardillo, M. J. *J. Chem. Phys*. **1980**, *72*, 1039. Tully, J. C. *J. Chem. Phys*. **1990**, *92*, 680.

(41) The lowest frequencies are propane (200 cm^{-1}), propene (428 cm^{-1}), acetaldehyde (525 cm^{-1}), formic acid (625 cm^{-1}), dimethyl ether (203 cm^{-1}), and ethanol (433 cm^{-1}).

(42) Belousov, V. P.; Panov, M. Y. *Thermodynamic Properties of Aqueous Solutions of Organic Substances*; CRC Press: Boca Raton,FL, 1994; Table III. *J. Phys. Chem. Ref. Data* **1982**, *11* (Suppl. 2). Cabini, S.; Gianni, P.; Mollica, V.; Lepori, L. *J. Solution Chem*. **1981**, *10*, 563. Wilhelm, E.; Battino, R.; Wilcock, R. J. *Chem. Rev*. **1977**, *77*, 219.

(43) Lipkin, N.; Gerber, R. B.; Moyseiv, N.; Nathanson, G. M. *J. Chem. Phys*. **1994**, *100*, 8408.

(44) Gillespie, R. J. *J. Chem. Soc*. **1950**, 2542. Gillespie, R. J.; Wasif, S. *J. Chem. Soc*. **1953**, 221.

(45) A fraction of the species may be present as zwitterions, $CH_3CH_2O(H^+)OSO_3^-$. Miller, G. P., personal communication.

(46) Jaques, D.; Leisten, J. A. *J. Chem. Soc*. **1961**, 4963. Burwell, R. L. *Chem. Rev*. **1954**, *54*, 615.

(47) Olah, G. A.; O'Brien, D. H. *J. Am. Chem. Soc.* **1967**, *89*, 1725.

(48) Crotonaldehyde, $CH_3CH{=}CH_2CHO$, is reported to form at higher aldehyde concentrations. See: McTigue, P. T.; Gruen, L. C. *Aust. J. Chem.* **1963**, *16*, 177.

(49) Hoshino, S.; Hosoya, H.; Nagakura, S. *Can. J. Chem.* **1966**, *44*, 1961.

(50) DeRight, R. E. *J. Am. Chem. Soc.* **1933**, *55*, 4761.

(51) Extensive breakdown into $CO + H_2O$ occurs at longer times in an oscillatory fashion when liquid formic acid is mixed with sulfuric acid. The unimolecular dissociation constant is reported to be 5×10^{-4}/s. See: Smith, K. W.; Noyes, R. M.; Bowers, P. G. *J. Phys. Chem.* **1983**, *87*, 1514.

(52) $\Delta H \approx -50$ kJ/mol for $3CH_3CH{=}CH_2 + 2H_2SO_4 \leftrightarrow (CH_3)_2CHOSO_3H + [(CH_3)_2CHO]_2SO_2$. See: *Ullmann's Encyclopedia of Chemistry*; Elders, B., Ed.; VCH: New York, 1993; Vol.. A22, p 176.

(53) The apparent activation energy for absorption of 2-butene, which forms a tertiary carbonium ion, is 55 kJ/mol in 50−71 wt % H_2SO_4. The activation energy for hydration of propene in dilute perchloric acid is 110 kJ/mol. See: Gehlwat, J. K.; Sharma, M. M. *Chem. Eng. Sci*. **1968**, *23*, 1173. Baliga, B. T.; Whalley, E. *Can. J. Chem*. **1965**, *43*, 2453.

(54) Eigen, M. *Angew. Chem., Int. Ed. Engl.* **1964**, *3*, 1. Ando, K.; Hynes, J. T. *J. Mol. Liq*. **1995**, *64*, 25 and references therein.

(55) Williams, L. R., personal communication.

(56) Based on the solubility of ethanol in water from: Dobson, H. J. E. *J. Chem. Soc*. **1925**, 127.

(57) Hanson, D. R.; Ravishankara, A. R. *J. Phys. Chem.* **1993**, *97*, 12309.

(58) The continuum equation governing gas uptake onto a fresh surface, $\gamma(t)/\alpha = \mathrm{erfc}((t/\tau)^{1/2})e^{t/\tau}$, allows us to estimate the maximum time before reaction must occur to observe a maximum 1% desorption flux. In this case, $\gamma(t = t_{max})/\alpha = 0.99$ and t_{max}/τ is calculated to be 10^{-4} or $t_{max} \approx 10^{-11}$ s, implying a penetration distance of roughly 1 Å before protonation. This depth is smaller than the interfacial thickness and is not likely to be valid within the diffusion−solution model. However, the small estimated depth and physical solvation time suggest that protonation takes place in or very near the interface on a time scale of nanoseconds or less.